Published OnlineFirst November 7, 2011; DOI: 10.1158/0008-5472.CAN-11-2178

Cancer Research

# A Dynamic Inflammatory Cytokine Network in the Human Ovarian Cancer Microenvironment

Hagen Kulbe, Probir Chakravarty, D. Andrew Leinster, et al.

*Cancer Res* 2012;72:66-75. Published OnlineFirst November 7, 2011.

Published OnlineFirst November 7, 2011; DOI: 10.1158/0008-5472.CAN-11-2178



# A Dynamic Inflammatory Cytokine Network in the Human Ovarian Cancer Microenvironment

Hagen Kulbe[1], Probir Chakravarty[2], D. Andrew Leinster[1], Kellie A. Charles[1], Joseph Kwong[1], Richard G. Thompson[1], Jermaine I. Coward[1], Tiziana Schioppa[1], Stephen C. Robinson[1], William M. Gallagher[3], Laura Galletta[5] on behalf of the Australian Ovarian Cancer Study Group, Michael A. Salako[1], John F. Smyth[4], Thorsten Hagemann[1], Donal J. Brennan[3], David D. Bowtell[5], and Frances R. Balkwill[1]

## Abstract

Constitutive production of inflammatory cytokines is a characteristic of many human malignant cell lines; however, the *in vitro* and *in vivo* interdependence of these cytokines, and their significance to the human cancer microenvironment, are both poorly understood. Here, we describe for the first time how three key cytokine/chemokine mediators of cancer-related inflammation, TNF, CXCL12, and interleukin 6, are involved in an autocrine cytokine network, the "TNF network," in human ovarian cancer. We show that this network has paracrine actions on angiogenesis, infiltration of myeloid cells, and NOTCH signaling in both murine xenografts and human ovarian tumor biopsies. Neutralizing antibodies or siRNA to individual members of this TNF network reduced angiogenesis, myeloid cell infiltration, and experimental peritoneal ovarian tumor growth. The dependency of network genes on TNF was shown by their downregulation in tumor cells from patients with advanced ovarian cancer following the infusion of anti-TNF antibodies. Together, the findings define a network of inflammatory cytokine interactions that are crucial to tumor growth and validate this network as a key therapeutic target in ovarian cancer. *Cancer Res; 72(1); 66–75. ©2011 AACR.*

## Introduction

A majority of human malignant cell lines constitutively secrete cytokines and chemokines as a consequence of oncogenic mutations and disregulated signaling pathways (1). However, it is not clear whether this cytokine/chemokine expression has relevance to the regulation of complex human tumor microenvironments.

We previously reported that the cytokines TNF and interleukin (IL)-6, the chemokine CXCL12 and its CXCR4 receptor were constitutively expressed and coregulated in ovarian cancer cell lines in tissue culture (2, 3). Stable knockdown of TNF mRNA in one of these cell lines provided evidence for an autocrine cytokine network with paracrine actions on blood vessel development in a peritoneal xenograft model (3).

The aim of this study was to investigate whether this autocrine cytokine network was relevant to the human tumor microenvironment of ovarian cancer. We present evidence, for the first time, that the cytokine network exists in human cancer biopsies. TNF, CXCL12, and IL-6 are coexpressed and coregulated in human ovarian cancer biopsies in what we describe as the "TNF network." We show that high TNF network pathway gene expression in the tumor microenvironment associates with genes involved in angiogenesis, inflammation, leukocyte infiltrates, and NOTCH signaling. This was confirmed by inhibition of the TNF network in experimental ovarian cancer models and in tumor cells from ovarian cancer patients after infusion of an anti-TNF antibody.

## Materials and Methods

### Ovarian cancer cells

IGROV-1 high-grade serous ovarian cancer cells and TOV21G clear-cell cancer cells were cultured as described (3). All cell lines have undergone 16 loci STR authentication (LGC Standards) and were most recently authenticated in September 2011. The cells were cultured in RPMI-1640 10% fetal calf serum.

### Immunohistochemistry

Paraffin-embedded biopsies, tissue arrays, and xenografts were stained with antibodies for CXCR4 (MAB173; R&D

**Authors' Affiliations:** [1]Centre for Cancer and Inflammation, Barts Cancer Institute, Queen Mary University of London, Charterhouse Square; [2]Cancer Research UK, Bioinformatics and Biostatistics Service, London, United Kingdom; [3]UCD School of Biomolecular and Biomedical Science, UCD Conway Institute, University College Dublin, Belfield, Dublin, Ireland; [4]Edinburgh Cancer Research UK Centre, Western General Hospital, Edinburgh, United Kingdom; and [5]Peter MacCallum Cancer Institute, Department of Biochemistry and Molecular Biology, University of Melbourne, Melbourne, Australia

**Note:** Supplementary data for this article are available at Cancer Research Online (http://cancerres.aacrjournals.org/).

**Corresponding Author:** Frances R. Balkwill, Centre for Cancer and Inflammation, Barts Cancer Institute, Queen Mary University of London, Charterhouse Square, United Kingdom. Phone: 0-207-882-3851; Fax: 0- 207-882-3885; E-mail: f.balkwill@qmul.ac.uk

**doi:** 10.1158/0008-5472.CAN-11-2178

Published OnlineFirst November 7, 2011; DOI: 10.1158/0008-5472.CAN-11-2178



Systems), CXCL12 (MAB350; R&D Systems), TNF (MAB 610; R&D systems), IL-6 (SC-7920; Santa Cruz Biotechnology), F4/80 (MCA497; Serotec) CD68 (Dako), and HES1 (Sc-25392; Santa Cruz Biotechnology Inc.). Negative controls were isotype matched.

### Western blotting

Cell extract (15 μg) was run on an SDS 10% acrylamide gel and transferred to a nylon membrane. The membrane was blocked overnight (4°C in PBS with 0.1% Tween and 10% milk powder) and probed using the anti-JAG1 antibody (AF1272; R&D Systems). A horseradish peroxidase–conjugated secondary antibody was used for detection (1:5,000) dilution at room temperature for 1 hour. Protein concentration equivalence was confirmed by anti–β-actin antibody

### Flow cytometry

Cells were counterstained with fluorescein isothiocyanate (FITC)-conjugated secondary antibody (Sigma) and analyzed on a FACScan flow cytometer using CellQuest software (BD Pharmingen).

### Cytokine ELISA

Cells were plated at $3 \times 10^5$ cells per well, cell culture supernatants removed after 48 hours of culture and cytokine concentrations measured using Quantikine ELISA Kits (R&D Systems). Frozen tissue was ground in liquid nitrogen and lysed in Tris-HCl, pH 8/50 mmol/L/NaCl 150 mmol/L/1% Triton X-100/DTT 1 mmol/L/1× inhibitor mixture mix (Calbiochem)/100 μg/mL phenylmethylsulfonylfluoride. Protein concentrations were determined by Bradford assay (Rad Laboratories).

### Transfection of IGROV-1 cells

IGROV-1 cells were transfected with SUPER RNAi plasmids containing 2 different short hairpin RNA (shRNA) sequences targeting CXCR4, or a control plasmid containing scrambled RNA (IGROV-Mock) and isolated according to Brummelkamp and colleagues (4). Lipofectamine was used for transfection as described previously (3). For transient knockdown, the ON-TARGET plus SMART pool of oligos targeting *CXCR4* gene expression was transfected using Dharmafect1 transfection reagent (Dharmacon). SiCONTROL nontargeting siRNA pool served as control. Lentiviral vectors containing the luciferase reporter construct were as described (3).

### RNA extraction and real-time quantitative RT-PCR

RNA was extracted using Tri Reagent (Sigma) and treated with 10 U DNase (Pharmacia). DNase-treated RNA (2 μg) was reverse transcribed with M-MLV reverse transcriptase (Promega). Multiplex real-time reverse transcriptase (RT-PCR) analysis was done using premade TaqMan probes (FAM) and 18s rRNA [individually ventilated cages (VIC)] specific primers and probes with the ABI PRISM 7700 Sequence Detection System instrument and software (PE Applied Biosystems). Expression values were normalized ($\Delta C_t$) to 18s rRNA by subtracting the cycle threshold ($C_t$) value of 18s rRNA from the $C_t$ value of the experimental value.

### Peritoneal xenografts

SPF female nude mice (Cancer Research UK) 6 to 8 weeks of age, housed in sterile IVC were injected intraperitoneally with $5 \times 10^6$ cells. Twice weekly treatment (5 mg/kg i.p.) was with monoclonal antibody infliximab or nonspecific, Gamimune N polyclonal human IgG control. Bioluminescence imaging was carried out and blood vessels quantified as before (3).

### Microarray experiments

Total RNA was isolated using the standard TRIzol protocol and purified further with the RNeasy Kit (Qiagen). RNA was quantified using a 2100 Bioanalyzer (Agilent Technologies). Expression profiles of all specimens were compared with a commercial universal reference RNA (Clontech). The Affymetrix GeneChip Human Genome U133 Plus 2.0 arrays were used. Probe synthesis and microarray hybridization were carried out according to standard Affymetrix protocols.

### Microarray analysis

Three Affymetrix datasets were obtained in triplicate. The NCBI GEO accession number for the arrays is GSE 13763. Data were analyzed using Bioconductor 1.9 running on R 2.6.0. Probeset expression measures (5, 6) were calculated using the Affymetrix package's Robust Multichip Average (RMA) default method (7). Differential gene expression was assessed between control (IGROV-1 and IGROV-Mock) and shRNAi (I) and (II) replicate groups, using an empirical Bayes *t* test (limma package; ref. 6); *P* values were adjusted for multiple testing using the Benjamini–Hochberg method (8). Any probe sets that exhibited an adjusted *P* value of 0.05 were called differentially expressed. In addition, any probe sets that exhibited an absolute fold change of greater than 2 were used to generate a heatmap. Two-dimensional hierarchical clustering of expression data using differentially expressed genes across control and shCXCR4 (I) and (II) samples was done. Samples were clustered using a 1–Pearson correlation distance matrix and average linkage clustering. Genes were clustered using a Euclidean distance matrix and average linkage clustering. The NCBI GEO accession number for the cell lines is GSE 13763. The NCBI accession number for datasets from the ascites cells is GSE18681.

### Gene set enrichment analysis

Differentially expressed probes were selected on the basis of meeting criteria of false discovery rate (FDR) < 0.05. Probes were divided into positive and negative fold change lists and used to determine enrichment using GeneGO processes within MetaCore pathway tool (GeneGo, Inc.). The analysis employs a hypergeometric distribution to determine the most enriched gene set

The microarray datasets GSE6008, GSE3149, and GSE9899 were downloaded from the GEO website. Datasets GSE6008 and GSE3149 were merged using Bioconductor 1.9 running on R 2.6.0. Probeset expression measures were calculated using the Affymetrix package's RMA default method. The microarray dataset from The Cancer Genome Atlas Network (TCGA) comprising 590 biopsies of high-grade serous ovarian cancer was downloaded from the TCGA data portal site (9).

Published OnlineFirst November 7, 2011; DOI: 10.1158/0008-5472.CAN-11-2178



The function GeneSetTest from the limma package was used to assess whether each sample had a tendency to be associated with an up- or downregulation of members of the, for example, TNF pathway. The individual genes in the TNF, CXCL12, and IL-6 pathways, as defined by MetaCore, are listed in Supplementary Table S1. Fourteen percent of the genes are shared among the 3 pathways. The function employs a Wilcoxon *t* test to generate *P* values. All samples were ranked on this enrichment, from the most significant to the least significant. The top and bottom 50 samples were extracted from the dataset as "high-TNF" and "low-TNF." The same process was used to identify samples that were enriched with members of the CXCL12 and IL-6 pathway. We also used immune cell-specific signatures (10).

### Patients and clinical trial design

The phase I/II trial was a single center, open-label, study of infliximab at 2 dose levels (5 mg/kg and 10 mg/kg) in patients with advanced epithelial ovarian cancer; full details in Charles and colleagues (11).

### Tissue microarray, image analysis, and cell counting in biopsies

Fifty-three cases of stage III/IV high-grade serous tumors were used for tissue microarray (TMA) construction as described in Brennan and colleagues (12), 4 cores per patient. The Aperio ScanScope XT Slide Scanner (Aperio Technologies) system was used to capture whole slide digital images with a 20× objective. Slides were dearrayed to visualize individual cores, using Spectrum (Aperio). Genie histology pattern recognition software (Aperio) was used to identify tumor from stroma in individual cores, and a color deconvolution algorithm (Aperio) was used to quantify TNF, CXCL12, and IL-6. For assay of $CD68^+$ cells in the Australian Ovarian Cancer Study (AOCS) ovarian cancer biopsies, microscope fields that contained tumor and adjacent stroma were counted blind at ×40 magnification.

### Ethics

The clinical study was approved by North East London and the City Health Authority Research Ethics Committee (LREC P/02/150) and Lothian Research Ethics Committee (LREC2000/4/60, LREC/2002/8/31) and conducted according to the declaration of Helsinki. All patients gave voluntary, written informed consent. The TMA study was approved by the Research Ethics Committee at the National Maternity Hospital, Dublin, Ireland. Access to human biopsy samples satisfied requirements of the East London and City Health Authority Research Ethics Subcommittee (LREC number 07/Q0604/25).

### Statistical analysis

Statistical analysis of *in vitro* and animal experiments used 1-way ANOVA, $\chi^2$ test, or unpaired *t* test with Welch correction (GraphPad Prism version 4 Software).

## Results

### Evidence for a cytokine network in ovarian cancer biopsies

Using gene expression microarray datasets from ovarian cancer biopsies in which more than 90% of samples were stage III/IV high-grade serous cancer, we first looked for associations between gene expression levels of the TNF, CXCL12, and IL-6 signaling pathways. Biopsies from the AOCS were ranked by expression levels of genes in the TNF, CXCL12, and IL-6 signaling pathways in each sample relative to the mean levels of gene expression in all samples (Method, Supplementary Fig. S1; individual genes in TNF, CXCL12, and IL-6 pathways, Supplementary Table S1). The top 50 samples with the highest levels of gene expression were compared with the bottom 50 samples with the lowest levels of gene expression in the TNF, CXCL12, and IL-6 pathways, so that each sample was associated with 3 *P* values. Using a binomial distribution, we found that samples that were highly enriched in one pathway, that is, ranked in the top 50, were highly likely to have high expression levels of genes in the other 2 pathways (Table 1). We then merged 2 additional ovarian cancer gene expression microarray datasets to give another 245 ovarian cancer biopsy samples and also conducted the same analysis on the 590 biopsies of high-grade serous cancer from the TCGA dataset, this time analyzing those samples that were in the highest 25% and lowest 25% of samples. The associations between high

**Table 1.** Coexpression of TNF network signaling pathways in ovarian cancer biopsies

| Pathways enrichment | Pathways linked | AOCS dataset | Merged dataset | TCGA dataset |
|---|---|---|---|---|
| TNF | CXCL12 | $6.6 \times 10^{-32}$ | $3.6 \times 10^{-8}$ | $1.6 \times 10^{-11}$ |
| | IL-6 | $1.5 \times 10^{-25}$ | $3.8 \times 10^{-6}$ | $4.5 \times 10^{-13}$ |
| CXCL12 | TNF | $1.3 \times 10^{-20}$ | $1.1 \times 10^{-4}$ | $2.0 \times 10^{-9}$ |
| | IL-6 | $2.1 \times 10^{-25}$ | $1.3 \times 10^{-5}$ | $1.5 \times 10^{-16}$ |
| IL-6 | CXCL12 | $7.6 \times 10^{-33}$ | $6.7 \times 10^{-16}$ | $3.3 \times 10^{-17}$ |
| | TNF | $4.1 \times 10^{-25}$ | $3.0 \times 10^{-16}$ | $1.0 \times 10^{-9}$ |

NOTE: Comparison of the samples with the 50 "highest" versus the 50 "lowest" levels reveals an association between expression levels of genes in the TNF, CXCL12, and IL-6 signaling pathways in the AOCS ($n = 285$) and merged datasets ($n = 245$) and highest and lowest 25% of the TCGA samples ($n = 590$).

Published OnlineFirst November 7, 2011; DOI: 10.1158/0008-5472.CAN-11-2178



CXCL12, TNF, and IL-6 signaling pathway gene expression were fully validated (Table 1). The same significant associations were found if expression levels of individual receptor/ligand pairs, rather than pathways, were tested (data not shown). Hence, there was a 3-way interdependency of the cytokines in the human tumor biopsy samples, with the expression of each ligand and its signaling pathway related to the other.

### TNF, CXCL12, and IL-6 proteins colocalize in ovarian cancer biopsies

We used automated immunohistochemistry (IHC) to localize TNF, CXCL12, and IL-6 and determine whether the proteins were coexpressed at cellular level using a TMA of 53 cases of stage III/IV high-grade serous ovarian cancer (12). Using an automated algorithm, staining was expressed as a score that combined both the intensity and density of positive pixels and partitioned into epithelial and stromal fractions using image analysis software. In the malignant cell compartment, we found a significant association between expression of TNF and CXCL12 ($P < 0.004$) as well as between TNF and IL-6 ($P < 0.05$). There was also significant correlation between TNF levels in the stromal compartment and CXCL12 ($P < 0.004$) as well as between TNF and IL-6 (<0.001). We named the coexpression of these 3 mediators the TNF network.

### Further confirmation of the TNF network in cell lines

We previously reported that stable expression of shRNA to TNF inhibited CXCL12 and IL-6 production and CXCR4 expression in IGROV-1 cells (3). To look for further *in vitro* evidence of the TNF network, we stably expressed shRNA to CXCR4 in these cells (Fig. 1A). This also reduced constitutive production of TNF, CXCL12, and IL-6 (Fig. 1B) but did not affect production of TGF-β1 or basic fibroblast growth factor. Transient transfection of RNAi to CXCR4 in IL-6 and TNF producing TOV21G clear-cell carcinoma cells also attenuated TNF and IL-6 expression (Supplementary Fig. S2).

### Functional interdependence of TNF network cytokines

We then compared gene expression patterns in high and low TNF network biopsies and the IGROV-1 cells to obtain information on the actions of the TNF network. We prepared in triplicate microarrays from the mock transfected and shCXCR4 IGROV-1 cell lines described in Fig. 1A and B in which the TNF network was inhibited. An eBayes *t* test was used to determine a list of differentially expressed probes between IGROV1 cells treated with shCXCR4 versus IGROV-1 controls. The heatmap in Fig. 1C shows a hierarchical clustering using probes differentially expressed in shCXCR4 IGROV-1 cells compared with control/mock transfected IGROV-1 cells. We next selected gene expression data from biopsies that were in the highest or lowest 50 for gene

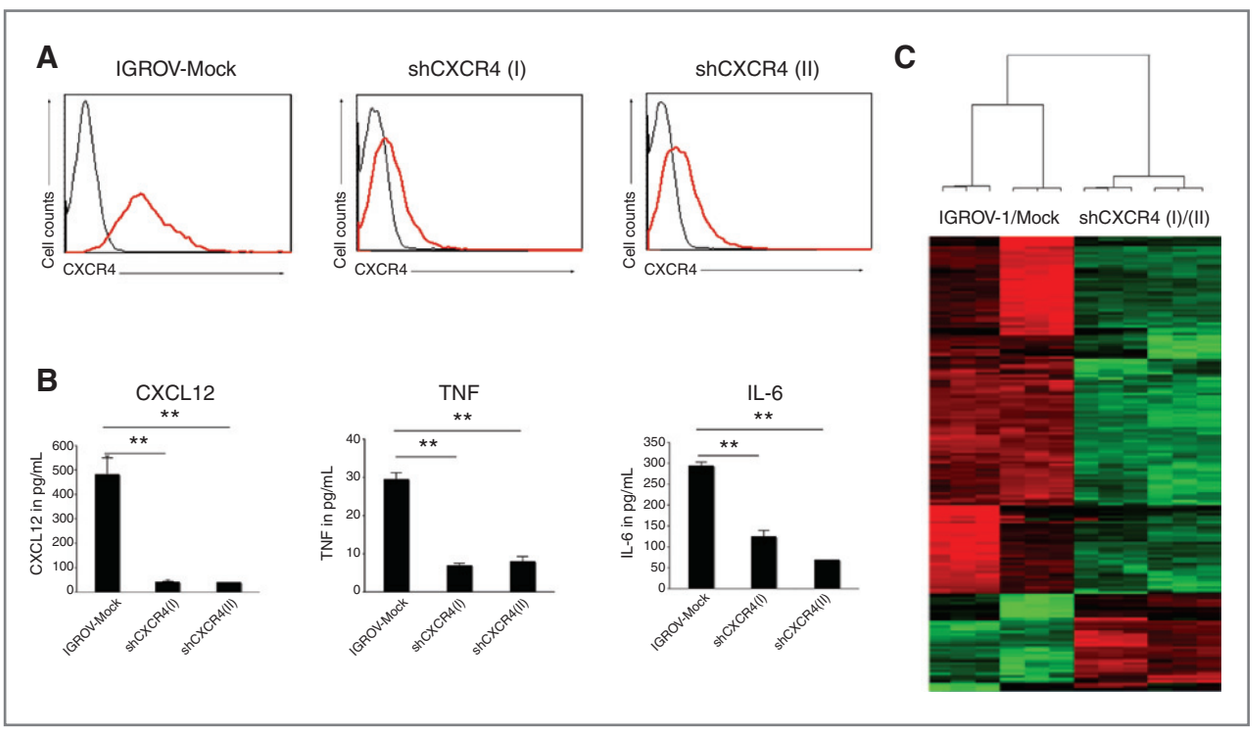


Figure 1. The TNF network and gene expression *in vitro*. A, cell surface expression of CXCR4 in IGROV-1 cells; IgG2α isotype control (black line), CXCR4 (red line). B, effects of CXCR4 knockdown on cytokine secretion by IGROV-1 ovarian cancer cells mean values (± SD) from triplicate wells (**, $P < 0.01$ as compared with IGROV-Mock cells). A and B, representative of 3 separate experiments. C, Affymetrix cDNA array analysis was done on IGROV-1 and IGROV-Mock transfected versus 2 independent IGROV-1 clones stably transfected with CXCR4 shRNA (I and II). Statistically different increases in gene expression are shown as pseudocolor red and green as decreases in expression.

Published OnlineFirst November 7, 2011; DOI: 10.1158/0008-5472.CAN-11-2178



**Table 2.** Pathways and processes that correlate with the TNF network

| | High versus low TNF network | | |
|---|---|---|---|
| **Pathways and processes** | **AOCS dataset** | **TCGA dataset** | **shCXCR4** |
| Development regulation of angiogenesis | 0.0007 | <0.0001 | <0.0001 |
| Cell adhesion | <0.0001 | <0.0001 | <0.0001 |
| NOTCH signaling | 0.0003 | 0.007 | 0.0003 |
| Cytoskeleton actin filaments | 0.0051 | <0.0001 | 0.0001 |
| Inflammation MIF signaling | 0.0007 | <0.0001 | 0.0021 |
| Development blood vessel morphogenesis | 0.0004 | <0.0001 | 0.0026 |
| Muscle contraction | 0.0002 | 0.0002 | 0.004 |
| Androgen receptor signaling | 0.003 | 0.003 | 0.004 |
| Inflammation protein C signaling | 0.007 | <0.0001 | 0.0081 |
| Cell adhesion cell junctions | <0.0001 | 0.018 | 0.0087 |
| Cell cycle | <0.0001 | <0.0001 | 0.009 |
| Immune cell signatures | <0.0001 | <0.0001 | N/A |

NOTE: The most significant pathways and processes were determined by the criteria of *P* value $P < 0.01$. Column 1 = high TNF network versus low TNF network samples from AOCS dataset; Column 2 = high TNF network versus low TNF network TCGA dataset; column 3 = IGROV-1 wild type and IGROV-1 mock versus 2 clones of shCXCR4 knockdown cells each parameter analyzed in triplicate.

expression levels for all 3 signaling pathways ($n = 28$ high TNF network biopsies, $n = 25$ low TNF network biopsies) from the AOCS dataset.

We then identified, using gene set enrichment analysis (GSEA; ref. 13), pathways and processes significantly increased in the high TNF network biopsies and cell lines compared with low TNF biopsies and cell lines, pathways and processes that were also significantly reduced in the cell lines when the network was inhibited by shRNA to CXCR4. We validated the results using the TCGA dataset, this time comparing 52 high TNF network samples versus 45 low TNF network samples defined as above for AOCS samples.

GSEA revealed a strong association between high TNF network expression and angiogenesis, cell adhesion, cell cycle, and inflammation signaling (Table 2). Strikingly, there was also a significant association with NOTCH signaling. As the biopsies would also contain infiltrating leukocytes, we looked for associations with immune cell signatures (10). High TNF network biopsy samples had significant enhancement of gene expression profiles for T cells, neutrophils, myeloid cells, monocytes, dendritic, and B cells ($P < 0.0001$) but not NK cells ($P = 0.053$) compared with the low TNF network group (Table 2 column 1). The complete gene list associated with high TNF network in the IGROV-1 cell lines and biopsies is available in Supplementary Tables S2 and S3, respectively.

### Knockdown of TNF network *in vivo*

Stable knockdown of CXCR4 in the IGROV-1 cells was maintained when they were grown as intraperitoneal xenografts (Supplementary Fig. S3A). Levels of CXCL12 and TNF protein were significantly decreased in tumors derived from shCXCR4-transfected cells (Supplementary Fig. S3B), and IL-6 levels were also significantly reduced in the tumors (16 pg $\pm$ 13 pg/100 μg protein compared with mean 846 pg $\pm$ 70 pg/100 μg protein in mock transfected tumors).

Stable knockdown of CXCR4 inhibited growth of peritoneal ovarian cancer xenografts measured by bioluminescence imaging (Fig. 2A), although it had no effect on cell growth *in vitro* (data not shown). Median survival of mice injected with IGROV-Mock cells was 46 days in contrast to 92 and 79 days in mice bearing tumors derived from 2 different clones of IGROV-shCXCR4 cells ($P < 0.0001$; Fig. 2B). The number of tumor deposits and the extent of organ involvement were significantly reduced in mice injected with IGROV-shCXCR4 cells ($P < 0.0001$ for both parameters) after 42 days (data not shown). F4/80+ macrophages were significantly reduced comparing size-matched shCXCR4 and mock transfected tumors (Fig. 2C). The vascular area of size-matched tumor deposits was significantly reduced in IGROV-shCXCR4 compared with IGROV-Mock tumors ($P < 0.0001$; Fig. 2D).

### Antibodies to TNF also inhibit angiogenesis and a myeloid cell infiltrate

The anti-human TNF antibody infliximab had similar actions to CXCR4 knockdown. After 4 weeks intraperitoneal growth and treatment *in vivo*, there was a reduction in tumor growth as evidenced by reduced luciferase expression in the anti-TNF–treated mice [Mean relative light units (RLU) of $1.1 \times 10^7$ and $1.1 \times 10^7$ for PBS and control IgG groups, respectively, compared with mean RLU $0.3 \times 10^7$ for anti-TNF–treated mice]. The vascular area and the F4/80+ infiltrate were significantly reduced following anti-TNF treatment (Fig. 3A and B). There was also a reduction in IL-6 protein as assessed by IHC in the tumors treated with anti-TNF antibodies (Fig. 3C).

### TNF network and the myeloid cell infiltrate in human biopsies

As the TNF network associated with the myeloid cell infiltrate, we asked whether TNF network gene expression

Published OnlineFirst November 7, 2011; DOI: 10.1158/0008-5472.CAN-11-2178



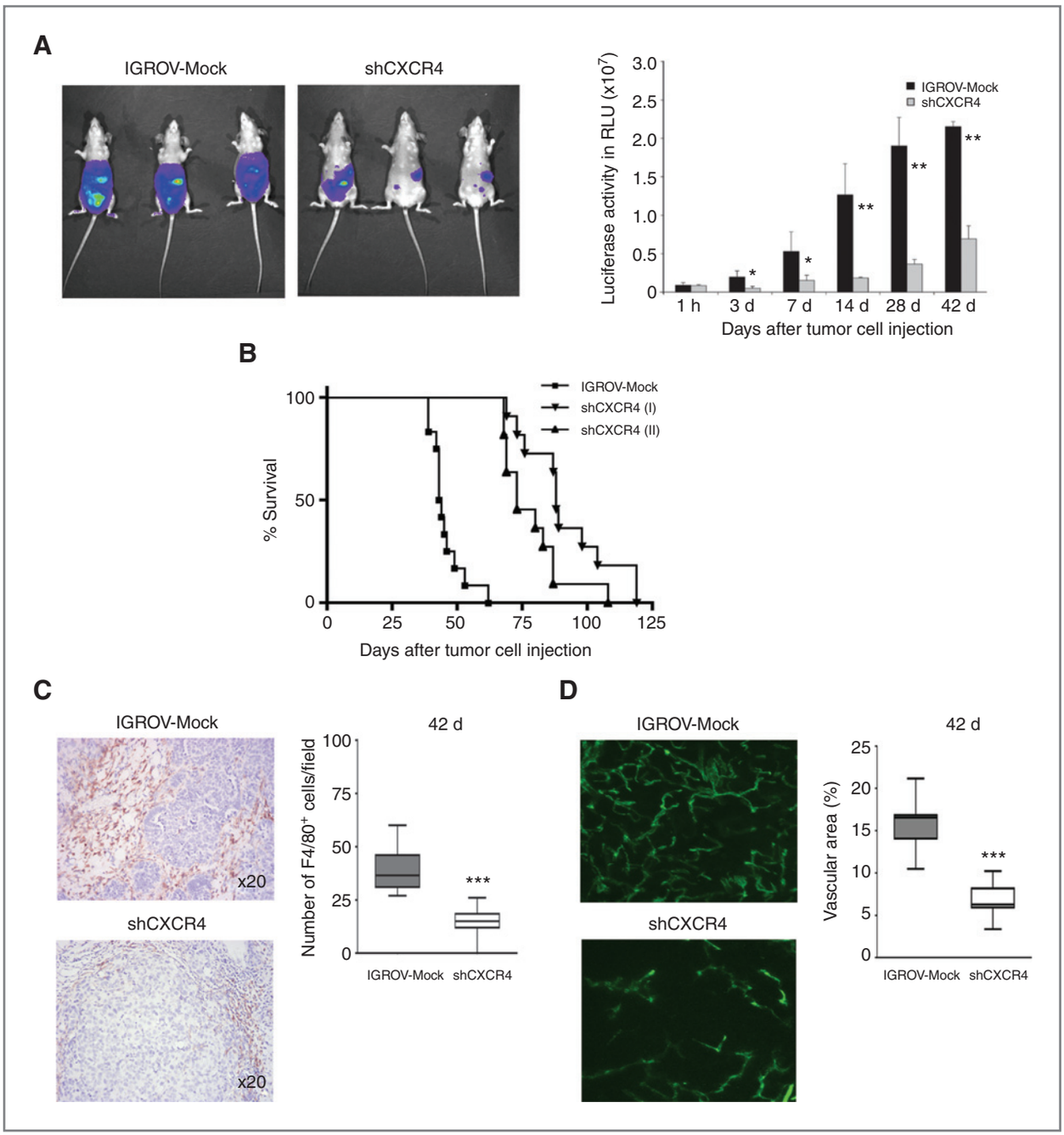


**Figure 2.** TNF network inhibition by shCXCR4 in ovarian cancer xenografts. A, bioluminescence imaging 42 days after intraperitoneal injection of IGROV-Mock, and IGROV-shCXCR4 luciferase expressing cells. Red, highest photon flux; blue, lowest photon flux. Quantification of bioluminescence from primary tumors ($n = 6$ mice per group; *, $P < 0.05$ and **, $P < 0.01$). B, survival of mice injected with ovarian cancer xenografts. Ten mice per group were injected with IGROV-Mock (squares), IGROV-shCXCR4 (I) (triangles), or IGROV-shCXCR4 (II) (inverted triangles) cells. Combined data from 2 separate experiments, $P < 0.0001$, both lines of IGROV-shCXCR4 compared with mice injected with IGROV-Mock cells. C, F4/80+ macrophages in the tumors. Graph represents number of macrophages quantified in 10 randomly selected areas (HPF ×40) of tumor sections ($n = 5$ each group) at 42 days (***, $P < 0.001$). D, angiogenesis evaluated 42 days after tumor cell injection. Confocal images (magnification, ×20) shown here are representative sections from tumors following injection of FITC-conjugated lectin and quantification of vascular area. Columns, mean vascular area in each group quantified in 10 randomly selected areas of tumor sections (mean ± SEM; **, $P < 0.01$). HPF, high power field.

correlated with myeloid cells in human tumor biopsies. We obtained 21 high-grade serous ovarian cancer biopsies from the AOCS series that matched those used in the analyses of Tables 1 and 2; 7 were from high and 14 from low TNF network biopsies. There was a striking association between $CD68^+$ macrophages in the stromal areas and high TNF

Published OnlineFirst November 7, 2011; DOI: 10.1158/0008-5472.CAN-11-2178



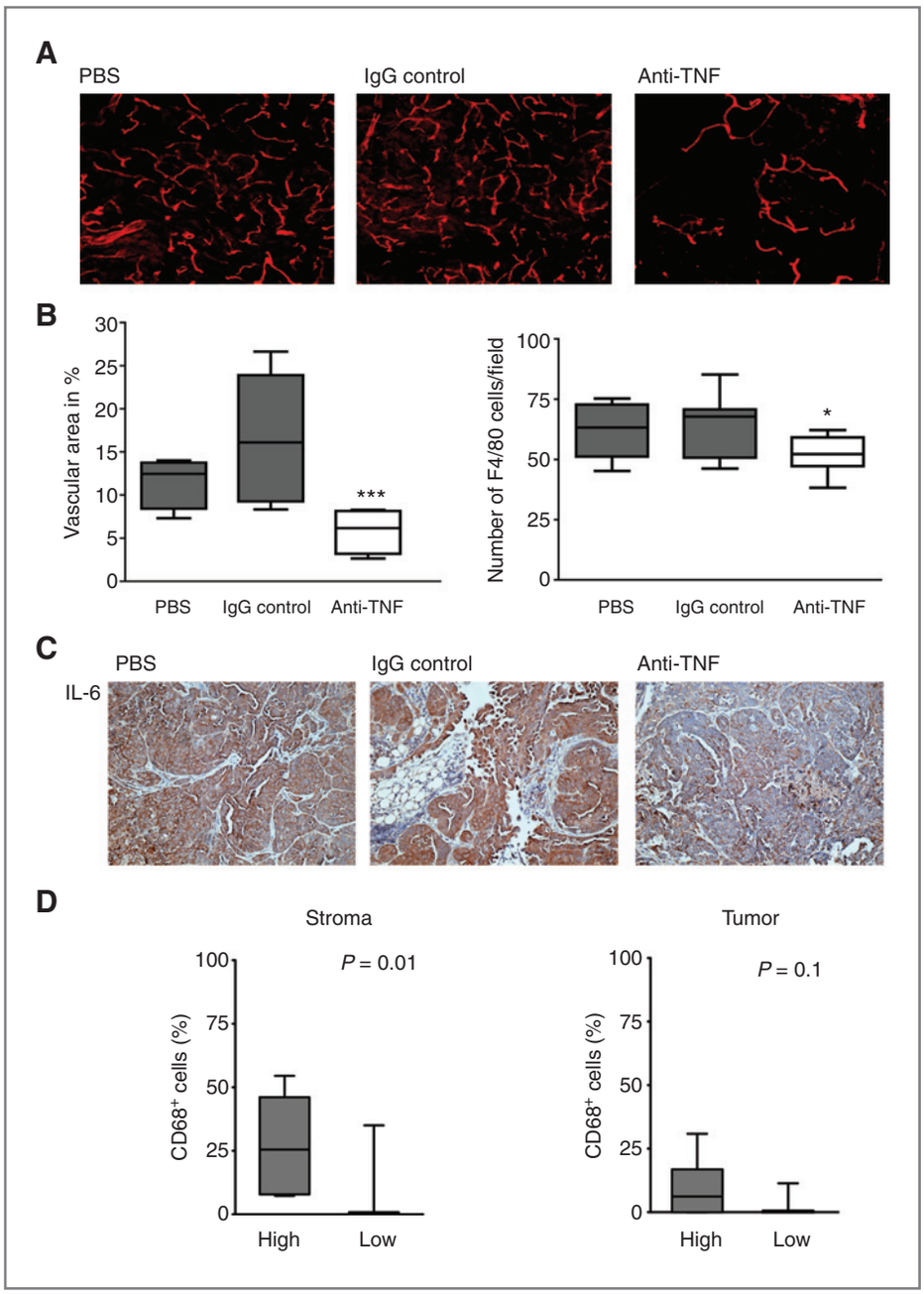


**Figure 3.** The TNF network, angiogenesis, and the myeloid cell infiltrate. A, treatment with anti-human TNF-$\alpha$ antibody infliximab influences tumor angiogenesis 28 days after tumor cell injection. Confocal images (magnification, $\times$20) of representative sections from tumors after injection of TRITC-conjugated lectin and B, quantification of the vascular area. Columns, mean vascular area in each group quantified in 10 randomly selected areas of tumor sections (mean $\pm$ SEM; ***, $P < 0.01$) and number of macrophages in each group quantified in 10 randomly selected areas (HPF $\times$40) of tumor sections ($n = 5$ each group) at 28 days (mean $\pm$ SEM; *, $P < 0.05$). C, IL-6 protein after treatment with infliximab. D, correlation between high TNF network gene expression in human high-grade serous ovarian cancer biopsies and CD68$^+$ cells. HPF, high power field.

network expression ($P = 0.01$; Fig. 3D). In 10 of 14 of the low TNF network biopsies, no CD68$^+$ cells could be detected in either tumor or stromal areas at all, whereas 7 of 7 high TNF network biopsies had visible CD68$^+$ cells.

### NOTCH signaling is correlated with the TNF network

To further investigate the association between the TNF network and NOTCH signaling (Table 2), we focused on NOTCH3 and JAG1 as both have been implicated in ovarian cancer (14, 15).

In the AOCS dataset, high TNF, CXCL12, and IL-6 signaling pathway expression significantly associated with JAG1 ($P = 0.03$; $P = 7.7 \times 10^{-7}$; $P = 0.00053$, respectively) and high CXCL12 and IL-6 with NOTCH3 ($P = 0.00016$; $P = 0.0044$, respectively). In IGROV-1 cells, NOTCH3 and JAG1 mRNA expression was significantly diminished when the TNF network was inhibited by shRNA to CXCR4 (Fig. 4A). Anti–IL-6 antibodies reduced constitutive JAG1 expression in IGROV-1 as well as in the TOV21G cells. Exogenous IL-6 stimulated JAG1 mRNA expression in a STAT3-dependent manner, and the

Published OnlineFirst November 7, 2011; DOI: 10.1158/0008-5472.CAN-11-2178



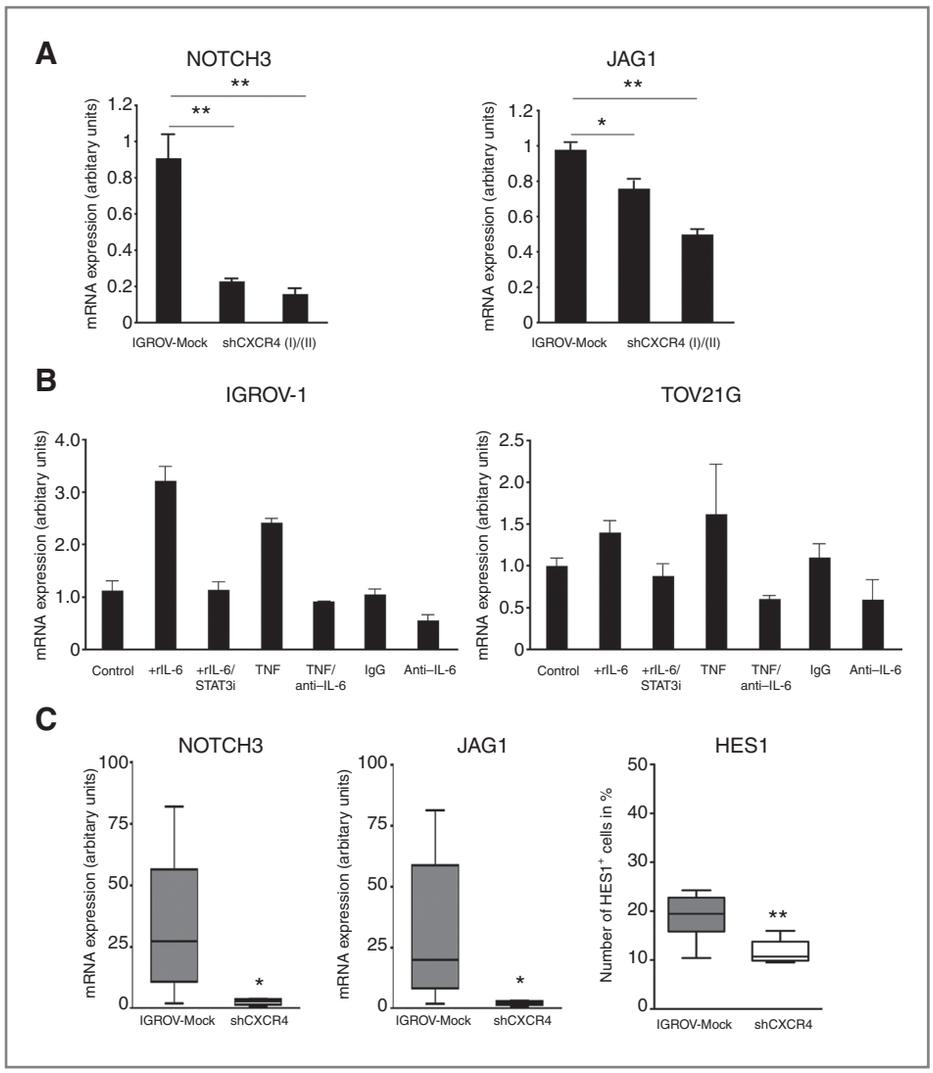


**Figure 4.** NOTCH signaling and the TNF network in ovarian cancer cells. A, levels of NOTCH3 mRNA in IGROV-Mock or IGROV-shCXCR4 cells and validation of the microarray gene expression analysis of JAG1 by real-time RT-PCR. Three samples in each group were used and *in vitro* mRNA expression levels in shCXCR4 cells compared with mock transfected cells (*, $P < 0.05$; **, $P < 0.01$). B, IL-6–dependent expression of Jagged1 in ovarian cancer cell lines assessed by real-time RT-PCR after stimulation with either 20 ng/mL IL-6 (with or without 1 μmol/L Stat3 inhibitor WP1066), 20 ng/mL TNF, or TNF with 10 μg/mL anti–IL-6 antibody for 48 hours. Data representative of 3 independent experiments. C, real-time RT-PCR measurement of mRNA levels of NOTCH3 and JAG1 ($n = 5$ each group; *, $P < 0.05$; **, $P < 0.01$) and number of tumor cell nuclei showing positive staining for HES1 in 10 randomly selected areas per tumor section ($n = 3$; **, $P < 0.01$).

effects of TNF could be inhibited by anti–IL-6 (Fig. 4B). NOTCH3 and JAG1 mRNA levels were also reduced in the tumor lysates from IGROV-1 shCXCR4 tumors. The percent of cell nuclei that stained positive for the HES1 transcription factor, downstream of NOTCH signaling, was also significantly inhibited in sections from the shCXCR4 tumors compared with controls (Fig. 4C, Supplementary Fig. S3C). Treatment of tumors with the anti-TNF antibody also significantly reduced nuclear HES1 protein staining (Supplementary Fig. S4). We concluded that key members of the TNF network regulate NOTCH3, JAG1, and HES1.

### Anti-TNF treatment of patients with ovarian cancer

We then sought evidence that the TNF network could be inhibited in ovarian cancer patients. Serial samples of ovarian cancer ascites were obtained from 9 patients with advanced disease, who had been treated with the anti-human TNF antibody infliximab (11). We compared ascites cell TNF network gene expression levels pretreatment, 24 and 48 hours after infliximab infusion. The results are shown as a heatmap (Fig. 5A), with green indicating lower and red indicating higher expression relative to pretreatment. Four patients showed a significant downregulation of TNF network gene expression 24 and/or 48 hours after anti-TNF antibody infusion. We compared the global gene expression patterns in pretreatment tumors from patients who showed robust downregulation of the TNF network versus those with little attenuation (patients 1–4 vs. patients 5–9; Fig. 5A). An empirical Bayes *t* test (6) identified 280 probes that were significantly different between the groups (with an FDR of $P < 0.001$). Probes and samples were clustered with the 280 genes, using average linkage clustering to generate a hierarchical clustering heatmap (Fig. 5B). We tested whether the gene sets representing the TNF, CXCL12, and IL-6 pathways were enriched in either group. TNF ($P = 2.68 \times 10^{-9}$), CXCL12 ($P = 3.83 \times 10^{-9}$), and IL-6 ($P = 5.37 \times 10^{-7}$) pathways were statistically enriched in patients 1 to 4 compared with patients 5 to 9, as was NOTCH signaling ($P = 1.64 \times 10^{-3}$) and enhanced gene expression profiles of T cells,

Published OnlineFirst November 7, 2011; DOI: 10.1158/0008-5472.CAN-11-2178



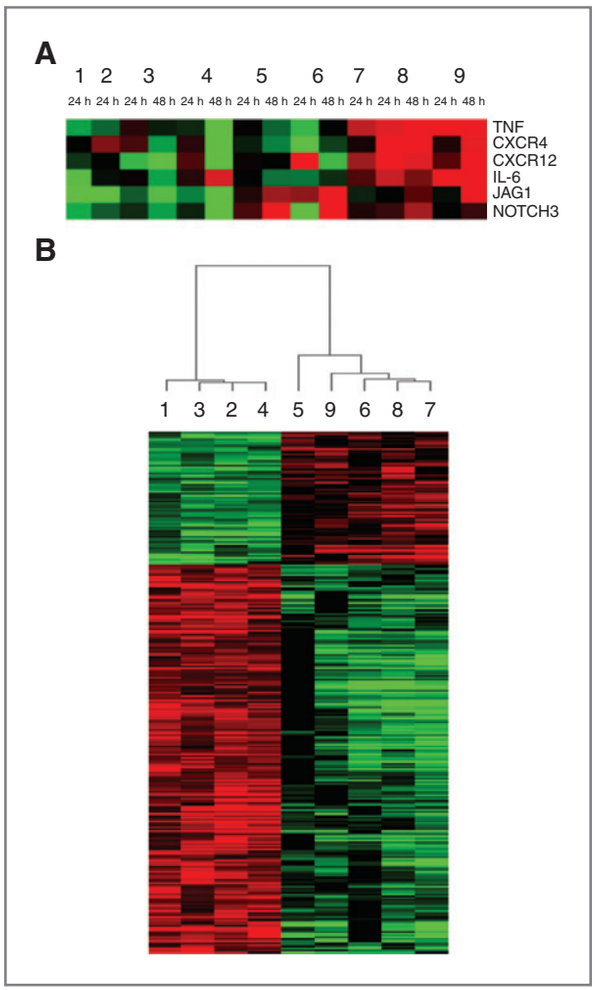


Figure 5. Effects on ascites cell gene expression during infliximab treatment. Serial ascites cell samples pretreatment and during treatment were obtained from 9 patients. Patients 1, 2, 5, 6, and 8 received 10 mg/kg and 3, 4, 7, and 9 received 5 mg/kg infliximab. A, RT-PCR results for the member of the TNF network shown in heatmap format. Red indicates higher expression and green indicates low expression relative to the mean expression of the gene across all samples. A Pearson's correlation was used to determine how similar the expression levels of the genes were to the expression profile of TNF. A correlation coefficient (cc) of 1 indicates an exact match (CXCR4, cc = 0.70; CXCL12, cc = 0.77; IL-6, cc = 0.72; JAG1, cc = 0.95, and NOTCH3, cc = 0.79). B, differential gene expression of the same 9 patient samples before treatment was assessed using an empirical Bayes *t* test. A total of 280 probes were found to be statistically significant. At a *P* value threshold of 0.001, these were used to draw a hierarchical cluster heatmap using Cluster.

neutrophils, myeloid, monocytes, dendritic, and B cells ($P < 0.0001$). Patients who had the highest level of TNF network expression showed the most intense downregulation of the network following infliximab anti-TNF antibody.

## Discussion

We have used a combination of molecular biology, bioinformatics, and cancer biology techniques to show that key pathways in cancer-related inflammation and Notch signaling are part of an autocrine malignant cell network in human ovarian cancer, a network with paracrine actions on angiogenesis and myeloid cell infiltration into tumors. The starting point of the current work was an observation in ovarian cancer cell lines (3). Here, we have found that information obtained from these cell lines is relevant to biopsies advanced human high-grade serous ovarian cancer. Our data also suggest that malignant cells regulate the inflammatory cytokine network in the human ovarian cancer microenvironment.

The factors coregulated in the TNF network have been individually considered as targets for cancer treatment. In 2 clinical studies of TNF antagonists in women with advanced ovarian cancer (11, 16), there was some evidence of transient disease stabilization and biological effects consistent with our knowledge of the actions of TNF. In a phase II trial of the anti–IL-6 antibody siltuximab in 18 patients with relapsed progressing ovarian cancer, there was one partial response, and 7 patients achieved periods of disease stabilization (17). In the context of the TNF network data described here, patients receiving siltuximab for 6 months had a significant decline in plasma levels of CXCL12.

The most common and lethal form of ovarian cancer is high-grade serous ovarian cancer (18). More than 95% of all the biopsies investigated (mRNA samples and biopsy sections) in our work were of this subtype. The IGROV-1 cell line is derived from a high-grade serous case. Clear-cell carcinoma of the ovary is characterized by overexpression of the IL-6–STAT3–HIF pathway (19) and has distinct genetic drivers compared with high-grade serous cancers (20, 21). TOV21G cells produced the highest levels of IL-6 but also produced other TNF network members. We recently found that 1 other high-grade serous and 6 clear-cell carcinoma cell lines constitutively coproduce TNF, CXCL12, and IL-6 (H. Kulbe, unpublished data). There are many examples in the literature of human tumor cell lines that produce TNF, IL-6, or CXCL12 but to our knowledge, few studies have assessed all 3 of these cytokines together. We believe it is likely that the TNF network is active in tumors with distinct genetic lesions.

Our data show that targeting cytokines, such as TNF and IL-6, is more likely to influence the tumor microenvironment than to kill malignant cells directly. Therefore anticytokine treatments, which are generally well tolerated in patients with inflammatory or malignant disease, are likely to be most useful in combination with conventional chemotherapy or treatments that target the malignant cell directly.

The TNF network defined here has features of a robust network as described by Yarden and colleagues for EGF–ERBB (22, 23). Further characterization of the TNF network using a systems biology approach may suggest new ways of treating the high-grade serous and clear-cell carcinoma. This approach may also help determine the best treatments to combine with anticytokine/chemokine agents. Because other malignant cell types produce TNF, IL-6, and CXCL12, these therapeutic strategies may be widely applicable in other cancers.

### Disclosure of Potential Conflicts of Interest

No potential conflicts of interest were disclosed.

Published OnlineFirst November 7, 2011; DOI: 10.1158/0008-5472.CAN-11-2178



## Grant Support

H. Kulbe, T. Schioppa, P. Chakravarty were funded by Cancer Research United Kingdom; J. Kwong was funded by AICR; D.A. Leinster and J. Kwong were funded by MRC; S.C. Robinson was funded by Barts and the London Charity, M.A. Salako was funded by Ovarian Cancer Action; T. Hagemann was funded by the MRC; R.G. Thompson and F.R. Balkwill were funded by HEFCE; and D.D. Bowtell is funded by the National Health and Medical Research Council of Australia, Cancer Councils of Australia, and the US Department of Defense Ovarian Cancer Research Program. The UCD Conway Institute is funded by the PRTLI administered by the Higher Education Authority of Ireland.

The costs of publication of this article were defrayed in part by the payment of page charges. This article must therefore be hereby marked *advertisement* in accordance with 18 U.S.C. Section 1734 solely to indicate this fact.

Received July 1, 2011; revised October 27, 2011; accepted October 27, 2011; published OnlineFirst November 7, 2011.

## References

1. Mantovani A, Allavena P, Sica A, Balkwill F. Cancer-related inflammation. Nature 2008;454:436–44.
2. Szlosarek PW, Grimshaw MJ, Kulbe H, Wilson JL, Wilbanks GD, Burke F, et al. Expression and regulation of tumor necrosis factor-alpha in normal and malignant ovarian epithelium. Mol Cancer Therapy 2006;5:382–90.
3. Kulbe H, Thompson RT, Wilson J, Robinson SC, Hagemann T, Fatah R, et al. The inflammatory cytokine TNF-alpha generates an autocrine tumour-promoting network in epithelial ovarian cancer cells. Cancer Res 2007;67:585–92.
4. Brummelkamp TR, Bernards R, Agami R. A system for stable expression of short interfering RNAs in mammalian cells. Science 2002;296:550–3.
5. Team RDC. R: A language and environment for statistical computing. R Foundation for Statistical computing 2008; ISBN 3-900051-07-0: Avalilable from: http://www.R-project.org
6. Smyth GK. Limma: linear models for microarray data. Bioinformatics and Computational Biology Solutions using R and Bioconductor 2005: 397–420.
7. Gautier L, Cope L, Bolstad BM, Irizarry RA. Affy-analysis of Affymetrix GeneChip data at the probe level. Bioinformatics 2004;20:307–15. Available from: http://bioconductor.org
8. Benjamini Y, Hochberg Y. Controlling the false discovery rate: a practical and powerful approach to multiple testing. J Roy Stat Soc, Ser B 1995;57:289–300.
9. Network TCGAR. Integrated genomic analyses of ovarian carcinoma. Nature 2011;474:609–15. Avaliable from: http://tcga-data.nci.nih.gov/tcga/
10. Abbas AR, Baldwin D, Ma Y, Ouyang W, Gurney A, Martin F, et al. Immune response *in silico* (IRIS): immune-specific genes identified from a compendium of microarray expression data. Genes Immun 2005;6:319–31.
11. Charles KA, Kulbe H, Soper R, Escorcio-Correia M, Lawrence T, Schultheis A, et al. The tumor-promoting actions of TNF-alpha involve TNFR1 and IL-17 in ovarian cancer in mice and humans. J Clin Invest 2009;119:3011–23.
12. Brennan DJ, Brandstedt J, Rexhepaj E, Foley M, Ponten F, Uhlen M, et al. Tumour-specific HMG-CoAR is an independent predictor of recurrence free survival in epithelial ovarian cancer. BMC Cancer 2010;10:125.
13. Subramanian A, Tamayo P, Mootha VK, Mukherjee S, Ebert BL, Gillette MA, et al. Gene set enrichment analysis: A knowledge-based approach for interpreting genome-wide expression profiles. Proc Natl Acad Sci U S A 2005;43:15545–50.
14. Park JT, Li M, Nakayama K, Mao TL, Davidson B, Zhang Z, et al. Notch3 gene amplification in ovarian cancer. Cancer Res 2006;15:6312–8.
15. Choi J-H, Park JT, Davidson B, Morin PJ, Shih I-M, Wang T-L. Jagged-1 and Notch3 juxtacrine loop regulates ovarian tumor growth and adhesion. Cancer Res 2008;68:5716–23.
16. Madhusudan S, Muthuramalingam SR, Braybrooke JP, Wilner S, Kaur K, Han C, et al. A phase II study of ethanercept (ENBREL) a tumour necrosis factor-alpha inhibitor in recurrent ovarian cancer. J Clin Oncol 2005;23:5950–9.
17. Coward J, Kulbe H, Chakravarty P, Leader D, Vassileva V, Leinster DA, et al. Interleukin-6 as a therapeutic target in human ovarian cancer. Clin Cancer Res 2011;17:6083–96.
18. Vaughan S, Coward J, Bast RCJr, Berchuck A, Berek JS, Brenton JD, et al. Rethinking ovarian cancer: recommendations for improving outcomes. Nat Rev Cancer 2011;11:719–25.
19. Anglesio MS, George J, Kulbe H, Friedlander M, Rischin D, Lemech C, et al. IL6-STAT3-HIF signaling and therapeutic response to the angiogenesis inhibitor sunitinib in ovarian clear cell cancer. Clin Cancer Res 2011;17:2538–48.
20. Bowtell DD. The genesis and evolution of high-grade serous ovarian cancer. Nat Rev Cancer 2010;10:803–8.
21. Wiegand KC, Shah SP, Al-Agha OM, Zhao Y, Tse K, Zeng T, et al. ARID1A mutations in endometriosis-associated ovarian carcinomas. N Engl J Med 2010;363:1532–43.
22. Citri A, Yarden Y. EGF-ERBB signalling: towards the systems level. Nat Rev Mol Cell Biol 2006;7:505–16.
23. Bubil EM, Yarden Y. The EGF receptor family: spearheading a merger of signaling and therapeutics. Curr Opin in Cell Biol 2007;19:124–34.